Pigment epithelium-derived factor (PEDF) and PEDF-receptor in the adult mouse brain: Differential spatial/temporal localization pattern

Yolanda de Diego-Otero[1,2,3] 🔘 | Rosa María Giráldez-Pérez[4] | Elena Lima-Cabello[1] | Raúl Heredia-Farfan[1] | Rocío Calvo Medina[5] | Lourdes Sanchez-Salido[1] | Lucía Pérez Costillas[2,6]

[1]Research Laboratory, Hospital Civil, Institute of Biomedical Research in Malaga (IBIMA), Málaga, Spain

[2]Mental Health Clinic Unit, .Regional University Hospital, Hospital Civil, Málaga, Spain

[3]Research Unit, International Institute of Innovation and Attention to Neurodevelopment and Language, Málaga, Spain

[4]Cellular Biology, Physiology and Immunology Department, University of Cordoba, Edificio Charles Darwin, Córdoba, Spain

[5]Pediatric Clinic Unit. Regional University Hospital, Hospital Materno-Infantil Avd, Arroyo de los Angeles, Málaga, Spain

[6]Psychiatry and Physiotherapy Department, University of Malaga. Medical School, Málaga, Spain

Correspondence
Yolanda de Diego-Otero, Laboratorio de Investigación, Hospital Civil, Pabellón 6-Sot, 29011 Málaga, Spain.
Email: ydediego@yahoo.es

Abstract

Pigment epithelium-derived factor (PEDF) is a multifunctional protein which was initially described in the retina, although it is also present in other tissues. It functions as an antioxidant agent promoting neuronal survival. Recently, a PEDF receptor has shown an elevated binding affinity for PEDF. There are no relevant data regarding the distribution of both proteins in the brain, therefore the main goal of this work was to investigate the spatiotemporal presence of PEDF and PEDFR in the adult mouse brain, and to determine the PEDF blood level in mouse and human. The localization of both proteins was analyzed by different experimental methods such as immunohistochemistry, western-blotting, and also by enzyme-linked immunosorbent assay. Differential expression was found in some telencephalic structures and positive signals for both proteins were detected in the cerebellum. The magnitude of the PEDFR labeling pattern was higher than PEDF and included some cortical and subventricular areas. Age-dependent changes in intensity of both protein immunoreactions were found in the cortical and hippocampal areas with greater reactivity between 4 and 8 months of age, whilst others, like the subventricular zones, these differences were more evident for PEDFR. Although ubiquitous presence was not found in the brain for these two proteins, their relevant functions must not be underestimated. It has been described that PEDF plays an important role in neuroprotection and data provided in the present work represents the first extensive study to understand the relevance of these two proteins in specific brain areas.

KEYWORDS

age-dependent, brain, colocalization, mouse, PEDF, PEDFR, RRID: AB_2187173, RRID: AB_2165678, RRID

1 | INTRODUCTION

Pigment epithelium-derived factor (PEDF), a 50-KDa multifunctional protein, was discovered as a secretion product in the retina (Tombran-Tink, Chader, & Johnson, 1991). PEDF acts as a neurotrophic, anti-angiogenic, and antitumorigenic agent (Barnstable & Tombran-Tink, 2004; Bouck, 2002; Crawford et al., 2001; Garcia et al., 2004; Gettins, Simonovic, & Volz, 2002; Wang et al., 2003). Many studies have been carried out on the retina, where PEDF is highly expressed (Becerra et al., 2004; Perez-Mediavilla et al., 1998). PEDF acts on photorecep-tor survival (Cayouette, Smith, Becerra, & Gravel, 1999) and in avoiding the pathological invasion of new vessels (Amaral & Becerra, 2010; Dawson et al., 1999). Other studies have demon- strated that PEDF promotes retinal progenitor cell survival against oxidative stress via upregulation of UCP2 expression (Wang et al., 2019; Zhu et al., 2010). PEDF is present in most tissues and carries out many other important roles to regenerate damaged tissue (Baxter-Holland & Dass, 2018; Doll et al., 2003; Hoshina, Abe, Yamagishi, & Shimizu, 2010; Sugita, Becerra, Chader, & Schwartz, 1997; Yamagishi, Matsui, Kawaguchi, & Sata, 2010). PEDF is impor- tant in the maintenance and protection of the CNS inducing neurite-outgrowth by developing motor neurons (Houenou et al., 1999) and protecting hippocampal (DeCoster, Schabelman, Tombran-Tink, & Bazan, 1999) and cerebellar granule cells and motor neurons against glutamate toxicity (Bilak et al., 1999; Taniwaki et al., 1997). PEDF acts in the inhibition of apoptosis of cerebellar granule cells (Araki, Taniwaki, Becerra, Chader, & Schwartz, 1998) and in the renewal of neural stem cells (Andreu-Agulló, Morante-Redolat, Delgado, & Fariñas, 2009; Ramírez-Castillejo et al., 2006). Some works link the modulation of PEDF levels in cerebrospinal fluid (CSF) with mental and neurodegenerative pathologies (Castaño, Roher, Esh, Kokjohn, & Beach, 2006; Kuncl et al., 2002; Zhang et al., 2019). It has been shown that PEDF can attenuate memory deficits associated with these pathologies in animal models (Storozheva et al., 2006).

Currently, numerous functional studies on PEDF have been car-ried out to elucidate its mechanism of action. Studies have been focused on how PEDF blocks the adverse effects of oxidative agents (Yamagishi, Nakamura, Ueda, Kato, & Imaizumi, 2005; Yoshida et al., 2008; Zhao et al., 2018). Other studies have shown that PEDF could act through cell-surface interactions (Alberdi, Aymerich, & Becerra, 1999; Taniwaki et al., 1997; Wu, Notario, Chader, & Becerra,

1995). Several studies have demonstrated that PEDF is a membrane-linked protein with specific and high binding affinity for PEDF and phospholipase A (2) activity (Pang, Zeng, Fleenor, & Clark, 2007). One study has demonstrated that the liver might be the source of increased circulating PEDF linked to insulin resistance; however, this does not happen in adipose tissue (Moreno-Navarrete et al., 2013). A novel receptor protein has been proposed with high affinity to PEDF, named PEDFR (Notari et al., 2006). PEDFR is a new member of the patatin-like phospholipase domain-containing 2 (PNPLA2) family (Subramanian, Notario, & Becerra, 2010).

Despite extensive studies carried out in numerous laboratories, to date no significant immunohistochemical data regarding PEDF protein localization in the brain has been provided. Moreover, a description of PEDFR protein localization in the brain is also necessary due to the important relationship between these two proteins and its association with mental and neurodegenerative diseases, where PEDF might assume important roles in neuronal protection. The aim of this study has been to perform an in deep description of representative regions showing PEDFR and PEDF in mouse brain.

2 | METHODS

2.1 | Animals

In this study we used the FVB-129 mouse strain, including 2, 4, 6, 8, and 12 months old mice generously provided by Dr. B. Oostra's lab (Erasmus University Rotterdam) and 4 month old CB57 mice generously provided from our animal house at the University of Malaga. This study was approved by the Animal Care and Use Committee of the Regional Uni-versity Hospital in Malaga and the University of Malaga. All experimental protocols were approved and met the guidelines of the European Com-munities Council Directive (86/609/EEC), European Laws for Animal Research (European Communities Council Directives 2010/63/EU, 90/219/EEC, Regulation [EC] No.1946/2003) and Spanish laws for Ani-mal Experimentation and research use of Genetic Modified Organism (RD-53/2013 and RD-178/2004, Law 32/2007) regarding the handling of experimental animals and the Animal Welfare Committee of the University of Malaga. The mice were housed under controlled condi-tions of humidity and temperature, with free access to standard food and water and were provided with a 12 hr light/dark cycle.

2.2 | Antibodies

Commercial antibodies were used for the specific detection of PEDF, and PEDF receptor (PEDF-R). Goat polyclonal anti-PEDF was obtained from R&D system (Catalogue Number: AF1177. RRID: AB_2187173) The immunogen used to generate the PEDF antibody was E. coli-derived recombinant human Serpin F1/PEDF peptide (aa Asp44-Pro418), accession number #P36955, which was then puri-fied by mouse PEDF affinity chromatography. The specificity of this antibody was probed previously by western blotting according to the manufacturer's instructions (Western blotting was carried out on mouse tissue lysates using PVDF membranes, probed with 2 µg/ml of Goat Anti-Human/Mouse Serpin F1/PEDF Antigen Affinity-purified Polyclonal Antibody (Catalogue #AF1177). A unique specific band was detected at ~50 kDa, compared with the molecular weight, as was predicted for the molecular weight of the PEDF protein. For PEDFR immunostaining, a sheep polyclonal antibody was purchased from R&D Systems (Catalogue # AF5365. RRID: AB_2165678), this antibody has been raised against a recombinant mouse PEDFR pep-tide (rmPEDFR; aa 162-253; Accession Number Q8BJ56) and purified by mouse PEDFR affinity chromatography. Anti-PEDFR specificity was validated by western blotting according to manufacturer's instructions. Rabbit anti-beta actin (1:1000; ABM Catalogue number Y058699) was used as loading control. Biotin-conjugated rabbit anti-sheep IgG and swine anti-rabbit IgG secondary antibodies were obtained from Santa Cruz Biotechnology (Catalogue number. sc-2776) and Dako (Catalogue number E0353), respectively.

2.3 | Western blot analysis

Western blot analysis was performed on brain extracts (Figure S1). Brains from 2, 4, 6, and 12-month old male mice were dissected in main structures comprising the cortex (Ctx), hippocampus (Hi), cere-bellum (Cb), medial septal, and diagonal band nuclei (D). The Eye was also used as control. Samples were homogenized using a motorized pellet pestle in 1 ml of homogenization buffer containing 20 mM HEPES and 100 mM KCl pH 7.0 with protease inhibitor cocktails (SigmaFast, cat# 8830, Sigma, Saint Louis, MO). Protein concentration in each homogenized sample was measured by the Bradford method. Aliquots of tissue samples corresponding to 40 µg were heated to 100ºC for 5 min with an equivalent volume of sample buffer (con-taining 2% SDS and 5% mercaptoethanol, bromophenol blue, and 20% glycerol) and loaded onto 12% commercial polyacrylamide gels purchases from Biorad (Hercules, CA). Proteins were electro-transferred to a PVDF membrane, blocked for 1 hr at 37ºC in a block-ing solution containing 3% BSA, 0.05% Tween-20, and PBS (pH 7.4) and incubated overnight at 4ºC with primary antibodies in the block-ing solution. The following primary antibodies were used: goat anti-PEDF (1:100), sheep anti-PEDFR (1:50), rabbit anti-laminin (1:100) and rabbit anti-actin (1:1000) as control. The membranes were rinsed three times with 0.05% Tween-20 in PBS for 10 min each, followed by incubation for 1 hr at room temperature in a 1:5000 dilution of

mouse anti-goat or rabbit anti-sheep IgG-HRP (Santa Cruz Biotechnol-ogy, cat# sc-2354 RRID:AB_628490 and sc-2924 RRID:AB_656969, respectively) with 3% BSA in PBS. Each blot was washed three times for 10 min and then processed for analysis using an enhanced chemi-luminescence detection kit (catalogue number 170-5070. Biorad. Hercules, CA) and visualized with a digital luminescent image analyzer (Biorad Hercules, CA).

2.4 | Immunohistochemical procedure

Animals were deeply anesthetized with a mixture of ketamine and xylazine and fixed by vascular perfusion with 4% paraformaldehyde. Afterwards, fixed brains were embedded in 4% agar and sliced on a vibratome at 50 µm. Brain sections were incubated for 15 min in a mixture of PBS: methanol: hydrogen peroxide (8:1:1) for the inactiva-tion of endogenous peroxidase. Then, sections were washed with PBS and blocked with 10% normal serum (goat for PEDF and sheep for PEDFR assays), 0.3% Triton X-100 and 0.1% sodium azide for 1 hr. Subsequently, the slices were incubated overnight at room tempera-ture either with anti-PEDF 1:150 or anti-PEDFR 1:350 diluted in 5% normal serum (goat and rabbit, respectively), 0.3% Triton X-100 and 0.1% sodium azide. After three washes with PBS, the samples were incubated with secondary antibodies and diluted in the same diluents as the primaries. Sections were then washed with PBS and incubated with Extravidin-Peroxidase (Sigma, Cat. No. E-2886) and diluted in PBS with 0.3% Triton X-100 for 1 hr. The peroxidase reaction was detected by incubation with 0.05% (wt/vol) DAB, 0.05% (wt/vol) nickel ammonium sulphate and 0.1% (vol/vol) H_2O_2 in PBS. Sections were then washed and mounted on poly-lysined slides, dehydrated, covered with DPX mountant and a glass cover slip, then, dried (VWR, Cat. No. 360294H) and observed under a light photomicroscope. Sec-tions were analyzed and photographed using an Olympus BX61 microscope (Olympus, Tokyo, Japan). Brightfield photomicrographs were captured with a digital camera (DP70, Olympus, Japan). The sig-nals observed under the microscope were represented according to the amount of labeled cell bodies with more or less density of points in Schematic drawings of transverse sections through mouse brain included within the stereotaxic coordinates from bregma 1.98 mm to −6.12 mm, according to the mouse brain atlas (Franklin & Paxinos, 2007). The absence of secondary antibody cross-reaction was confirmed by the omission of the primary antibody from the immunohistochemical procedure. We ran the experiments on 16 male mice aged 2–12 months.

2.5 | Immunofluorescence procedure

The mice were sacrificed by cervical dislocation and blood samples were taken from the heart. The brains were extracted for study, intro-ducing them in liquid nitrogen and stored at −80ºC for their cryopres-ervation until use. Subsequently, samples were fixed in small pieces of tissue in 4% formaldehyde 3.7–4.0% buffered to pH = 7 for 48 hr

(252931.1315, Panreac Quimica SLU, Barcelona, Spain). Then placed in paraffin Spin Tissue Processor STP 120 (Myr, Tarragona, Spain) for 18 hr subjecting the tissues to successive passages on alcohols of increasing gradation, followed by xylol and paraffin. Finally, the blocks were made using a paraffin inclusion apparatus (EG1150H, Leica, Nussloch, Germany). Five micrometer slices were obtained with a microtome (RM2255, Leica, Nussloch, Germany) and mounted on treated slides (J1800AMNZ, Thermo Scientific Menzel-Gläser Superfrost Plus). Briefly, paraffin sections were deparaffinized after 20 min in an oven at 60ºC, followed by rehydration for histochemical or immunofluorescence procedures. Deparaffinized slides were then washed three times in PBS (pH 7.4), and subsequently an antigen unmasking solution was applied (H-3300, Vector, Burlingame CA), then incubated in a solution of 10% donkey serum (DS) (D9363, Merck KGaA, Darmstadt, German) and 10% albumin (AB) (S3772, Merck KGaA, Darmstadt, German) in PBS plus 0.3% Triton X-100 (Merck KGaA, Darmstadt, German, PBS+) for 1 hr. The sections were then incubated in a humid camera with a mix of primary Goat anti-PEDFR/PNPLA2/Desnutrin antibodies (1:75, catalogue number Y213921, Applied Biological Materials INC [abm], Richmond, BC, Canada) and Rabbit anti-SSERPINF1/PEDF (1:100, catalogue number Y400418, Applied Biological Materials INC [abm], Richmond, BC, Canada), overnight at 4ºC. The fluorescent labeled secondary anti-Goat IgG (H + L) FITC antibody produced in mouse (1:50, catalogue number 31512. RRID:AB_228369, Thermo Fisher Scientific, Rockford, IL) was diluted in PBS+ and 5% ABS, incubated at room temperature for 2,5 hr. Then slices were rinsed three times in PBS (10 min changes) and incubated at room temperature with Donkey anti-rabbit IgG (H + L) Rhodamine (1:50, catalogue number 31685, RRID:AB_429712, Thermo Fisher Scientific, Rockford, IL) diluted in PBS+ and 5% DS, incubated at room temperature for 2,5 hr and rinsed three times in PBS (10 min changes). The procedure was finalized with staining with Fluoroshield™ and DAPI (catalogue number F6057, Merck KGaA, Darmstadt, Germany) medium containing the fluorescent nuclear blue stain.

We verified the specificity of the antibodies used in the present work by two routine control procedures in some sections: omission of primary and secondary antibodies, and replacement of the different antisera with PBS. The fluorescence was checked with an Olympus BX61 microscope and a DP70 digital camera (Olympus, Tokyo, Japan). The sections were then photographed using a Confocal Leica microscope TCS SP8 and Leica LAS AF (Leica Microsystem, Wetzlar, Germany) software.

2.6 | PEDF detection in mouse serum and human plasma by ELISA technique

A total of 22 male mice of 2 ($n = 6$), 6 ($n = 5$), 8($n = 5$), and 12 ($n = 6$) months of age were sacrificed by cervical dislocation, then, blood was collected directly from the heart and, after clotting, samples were centrifuged at a low speed. Serum was separated into clean tubes and PEDF levels measured using a PEDF ELISA kit following the protocol instructions (CusaBio, cat# CSB-EO8820m). Briefly, samples were incubated in a microplate precoated with mouse PEDF, after that, a

biotin-anti-PEDF antibody was added in each well and samples were incubated at 37ºC. Anti-PEDF labeling was developed with HRP-avidin and absorbance at 450 nm was measured with a microplate reader.

PEDF levels were measured in a total of 18 plasma samples from human blood (2–5 years old $n = 6$; 9–15 years old $n = 6$, and 18–33 years old $n = 6$) with an ELISA kit following the protocol instructions (PEDF Sandwich ELISA Kit; Chemicon® International, Temecula, CA). The collection of all samples follow the ethical principles stated by the National Ethical Authority as well as International laws and ethical rules. The Institutional Research Board at the Regional University Hospital of Malaga reviewed the research protocol and the informed consent form for approval, adults and parents from children firm the approved informed consent. All the samples were obtained by graduated nurse following the principles of good practices from healthy controls, processes in less than 2 hr to obtain plasma that has been preserved at the Certified Regional Biobank located at the hospital. Briefly, blood samples were collected between 8:00 and 9:00 hr by venous puncture in commercial tubes containing EDTA (purchases from BD), and platelet-poor plasma was prepared by centrifugation (3,000 rpm, 20 min) and stored at −80ºC before use. To perform the assay, samples were thawed on ice and urea was added to a final concentration of 8 M. After incubation on ice for 1 hr, samples were diluted in assay diluent, then immediately applied to the specific PEDF ELISA assay plates and measured according to the stan- dard manufacturer's protocol.

2.7 | Quantification of positive immunoreactivity in cells

Quantitative studies of PEDF and PEDFR neurons in the cortex, hippocampus, ventricle, diagonal band nuclei, claustrum, and cerebellum were made on coronal sections of the 22 mice brain included within the stereotaxic coordinates bregma 1.98 to −6.12 mm according to the mouse brain atlas (Franklin & Paxinos, 2007), and the same atlas was used to delimit the borders of distinct nuclei, with 2,640 μm for periventricular area, 6,600 for Cortex, Claustro 4,440 μm for Claustrum nuclei, 1,200 μm for band diagonal nuclei and medial septal nucleus, 3,120 μm for Hippocampus and 1,200 μm for Cerebellum. The total number of immunoreactive cells in nuclei was estimated by means of the optical fractionator, which combines the optical dissector (Sterio, 1984) with a fractionator sampling scheme (Gundersen et al., 1988) following the method used by Giráldez-Pérez et al. (2013). An Olympus BX53 microscope and digital camera DP73 (Olympus, Tokyo, Japan) and Visiopharm's newCAST™ software package (Hoersholm Denmark) were used. The number of neurons was quantified in every fourth section (which accounts for 200 μm). A ×2 objective was used to delimit the nuclei and the quantity of cell bodies immunoreactive for PEDF or PEDFR was counted using a ×100/1.32 oil immersion objective. The quantification of the immunoreactive cells was carried out in the right part of the corresponding coronal sections. We used a step length of 375 × 375 μm at the cortex area

592 × 592 µm cortex 2, 693 × 693 µm cortex 3, 167 × 167 µm at the periventricular area, 188 × 188 at the layer CA1 of hippocampus, 198 × 198 µm for layer CA2-CA3 of hippocampus, 119 × 119 µm for claustrum areas, 117 × 117 µm for diagonal band nuclei and medial septal nucleus, and 180 × 180 µm for purkinje cerebellar layer. For all nuclei we used a counting frame of 356.2 µm^2. After having counted the objects (Σ Q$^-$), the total number of immunoreactivity cells was estimated as: N = Σ Q$^-$ x fs x fa x fh (Gundersen et al., 1988), where fs is the numerical fraction of the section used, fa is the areal fraction, and fh is the linear fraction of section thickness (Blasco et al., 1999). The coefficient of error (CE) for each estimation and animal ranged from 0.02 to 0.1. Differences in the number of immunoreactive cells are presented as the mean and *SD*. Moreover, the levels of significance between age groups and markers were statistically analyzed.

2.7.1 | Statistical analysis for quantification

Differences in the number of immunoreactive cells are presented as the mean ± *SD.* SPSS 24.0 and Sigma Stat software (SSPS, Chicago, IL) were used for all analyses. When a normal distribution of a variable was confirmed the means were compared using the unpaired *t*-test (for normally distributed populations), one way-analysis of variance (ANOVA) (for comparison of variance), and Bonferroni and Tukey post hoc tests. Non-normally distributed continuous variables were analyzed using the nonparametric Mann–Whitney test (statistical analysis of Elisa PEDF measurements). Values of *p* < .05 were considered to represent statistical significance.

3 | RESULTS

Although many studies have been carried out to understand the possible roles of PEDF and its receptor PEDFR in different tissues, few studies are dedicated to the systematic analysis of both proteins in the brain. This is the first systematic study devoted to analyze the distribution of PEDF and PEDFR in the mouse brain during aging.

3.1 | PEDF and PEDFR proteins detected by western blotting in several brain areas during aging in adult mouse

To understand the role of PEDF and PEDFR in the brain, protein detection by western blotting was performed. The antibodies used in this study specifically recognized the proteins in accordance with the predicted molecular weight. Homogenized samples from dissected areas of the brain (Cortex = Ctx, Cerebellum = Cb, Hippocampus = Hi, Medial Septum and Diagonal band nuclei = D) demonstrated that PEDF and PEDFR were present in all the areas, cortex, hippocampus, cerebellum, Medial Septum and Diagonal band nuclei (Figure 1). The eye homogenate was used as control for PEDFR (Figure 1a) and PEDF (Figure 1b), since the eye represented a well-known tissue expressing both these two
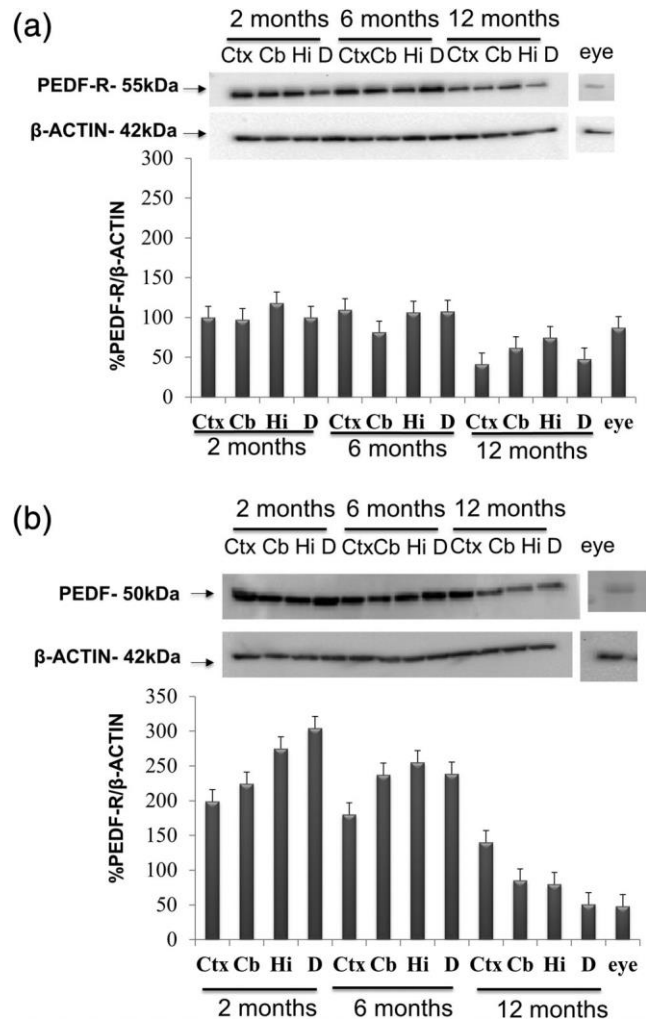
FIGURE 1 Western blot of homogenized dissected brain areas (Ctx, cortex; hip, hippocampus; Cb, cerebellum; D, Endopiriform dorsal nucleus) and eyes, a positive control for PEDF expression. PEDFR (a) and PEDF (b) showed a positive band with the expected molecular weight of 50 kDa for PEDF and 55 kDa for PEDFR along the adult stages, lower signal is detected in aged mouse brain for both proteins

proteins. A band was observed in both PEDF and PEDFR corresponding to the expected molecular weight, thus 55 kDa for PEDFR (Figure 1a) and 50 kDa for PDEF (Figure 1b). A significant reduction in the signal was observed for both proteins in all the studied areas in the 12 month old mouse group. Laminin receptor was also tested as it was identified as another PEDF receptor (Bernard et al., 2009), see Figure S1, a 67 kDa protein was detected and no significant difference was detected in the signal at the different area or ages.

3.2 | Immunohistochemical detection of PEDF and PEDFR proteins in the brain

To obtain a clear description of the presence of these proteins in the brain, a scheme of the immunodetected signal has been included in representative brain coronal sections to show the regions where

PEDF (red dots on the left brain scheme) and PEDFR (blue dots on the right brain scheme) give a clear and consistent positive staining (Figure 2A-f). Overall, the immunohistochemical results indicated the differential distribution of immunoreactive positive cells to PEDF and PEDFR proteins (Table 1 and Figures 2A and 2B). During adult aging, the main regions presenting the proteins are the telencephalon, cerebellum and periventricular area of the mouse brain in all the studied stages. Photographic composition from super photo, made with New Cast, of the corresponding sections of the schemes are included (Figures 2A and 2B).

A strong labeling was characteristic of the PEDFR positive cells. Cells showed a high and clustered cellular membrane staining surrounding a weaker labeled cytoplasm. The immunoreactivity was mostly localized in round-shaped and bipolar or multipolar cells. A noticeable labeling extended along all the cell body and the proximal dendrites (inserts in Figure 3b,d, and f) with the processes extending laterally. The comparative study between the different age groups using ANOVA analysis showed significant differences in the number of cells expressing PEDF and PEDFR, for all age groups (Table 1). Cells expressing PEDFR showed a significant higher number of positive cells than those expressing PEDF in 2 and 12 month old mice. In the case of the cerebellum for the age group between 4 and 8 months, an equal number of positive cells were observed with no significant differences. Statistical significance for ($p < .05$) (Table 1).

3.3 | Comparative distribution the PEDF and PEDFR immunoreactive cells in telencephalic structures

PEDFR immunoreactions were more intense and extended positive signal; stained cells covered more regions, than those found for PEDF. A low positive signal was found on PEDF in cells from the dorsal telencephalic regions (Figure 2A-left a–c). Only cingulate cortex and some septal nuclei of the ventromedial area were highly labeled. PEDF positive neurons were detected in the innermost layers of the prefrontal cortex (Figure 2A-left) around the forceps minor of corpus callosum, including the motor and sensory zone in the cortex. At rostral levels of the telencephalon, the labeling was mainly localized in the prefrontal cortex, surrounding the anterior extent of the corpus callosum, and areas of the ventral telencephalon (Figure 2A,B left). Medially, PEDFR cells were found along the medial wall of the telencephalon, including the cingulate cortex and prelimbic and infralimbic areas (Figure 2Aa–c right). Ventrally, the endopiriform nucleus presented positive cells disposed in a scattered fashion (Figure 2Aa–c right). PEDFR cells were also present in the claustrum, endopiriform nucleus with pyramidal morphology cells (Figures 2A-right and 3), and the shell of the nucleus accumbens (Figure 2A-right). The olfactory tubercle and septohippocampal nucleus also showed PEDF (Figure 2A-left) and PEDFR stained cells (Figure 2A-right).

Immunofluorescence experiments show colocalization of both proteins in some cells at the endopiriform nucleus, although PEDFR-expressing cells are a majority (Figure 3 and Table 1).

In addition, the shell region of the nucleus accumbens showed few and dispersed positive cells adjacent to the ventromedial part of the core (Figure 2A-right).

Immunoreactivity extends to the caudal area of the visual and piriform cortex (Figure 2A,B), it shows a positive signal for PEDF staining. PEDFR immunoreactions were more intense and stained cells covered more regions than PEDF (Figure 4a,c, and e). Caudally, a greater expression of PEDFR was distributed by the different cellular layers with higher density in the layers V and VI of the cortex (Figure 4b,d, and f). In addition, a greater expression was observed in mice of 4 to 8 months of age (Figure 4d and Table 1). A diffuse positive signal was mainly seen in the caudate putamen with some positive cells for PEDF (Figures 2B-c and 4a,c, and e). In the cortex, these results show that the number and the stain intensity of the positive PEDFR cells was higher in animals between the age of 4 to 8 months, compared to mice of 2 and 12 months old that show a similar staining pattern with a lower intensity (Figures 2B, 4 and Table 1). The different cell morphology according to the layer, pyramidal cells mostly in Layers V and VI, fusiform cells in Layer V and cells with starry morphology, mostly in layer III (Figure 4).

PEDFR labeling was also present in other extracortical structures. A generally low signal was detected in the amygdala (Figure 5b,d, and f), except for PEDFR expression between 2 and 8 months where a strong signal was detected (Figure 5b,d). A reduction in the immunohistochemical signal was found for PEDF and PEDFR in 12 month old mice in the amygdala (Figure 5e,f).

Positive cell bodies were also observed in the medial septal nucleus and positive cells were observed in the nucleus of the vertical limb of the diagonal band (VDB), and more laterally, in the nucleus of the horizontal limb of the diagonal band (HDB), mostly showing ovoid or fusiform morphology cells; PEDF-immunoreactive (Figures 2B and 6a,c, and e) and PDEFR-ir cells (Figures 2B and 6b,d, and f) were also present. The number of PEDFR positive cells was higher in all ages (Figure 6b,d, and f), the highest positive signal was recorded in 4/8 month old mice (Figure 6d). The immunofluorescence results displayed colocalization of some cells for both proteins in both VDB and HDB areas (Figure 3 and Table 1). There was a differential expression pattern in PEDFR in a time dependent manner in certain areas of the telencephalon.

This temporal pattern was also seen in the hippocampus, a neocortex brain area, with a maximum PEDFR expression in 4 to 8 month old mice (Figures 2A-c, B-d, and 7d), mostly finding pyramidal morphology cells. A diffuse signal, mainly in the CA1 and CA3 layers, was characteristic of all the studied animals and stages. Clusters of clear positive cell bodies were also shown in the CA1 layer (Figures 2A-c, 2B-d, and 7). This signal for PEDF was diffuse in the hippocampus (Figures 2A-c, B-d and 7a,c, and e) in all the animals analyzed, with a highly intense signal in CA1, CA2, and CA3 layers in 2 month old mice (Figure 7a), although in the quantification analyses, an increased number of cells expressing PEDFR than PDEF is observed in this age group (Figure 2A,B and Table 1).
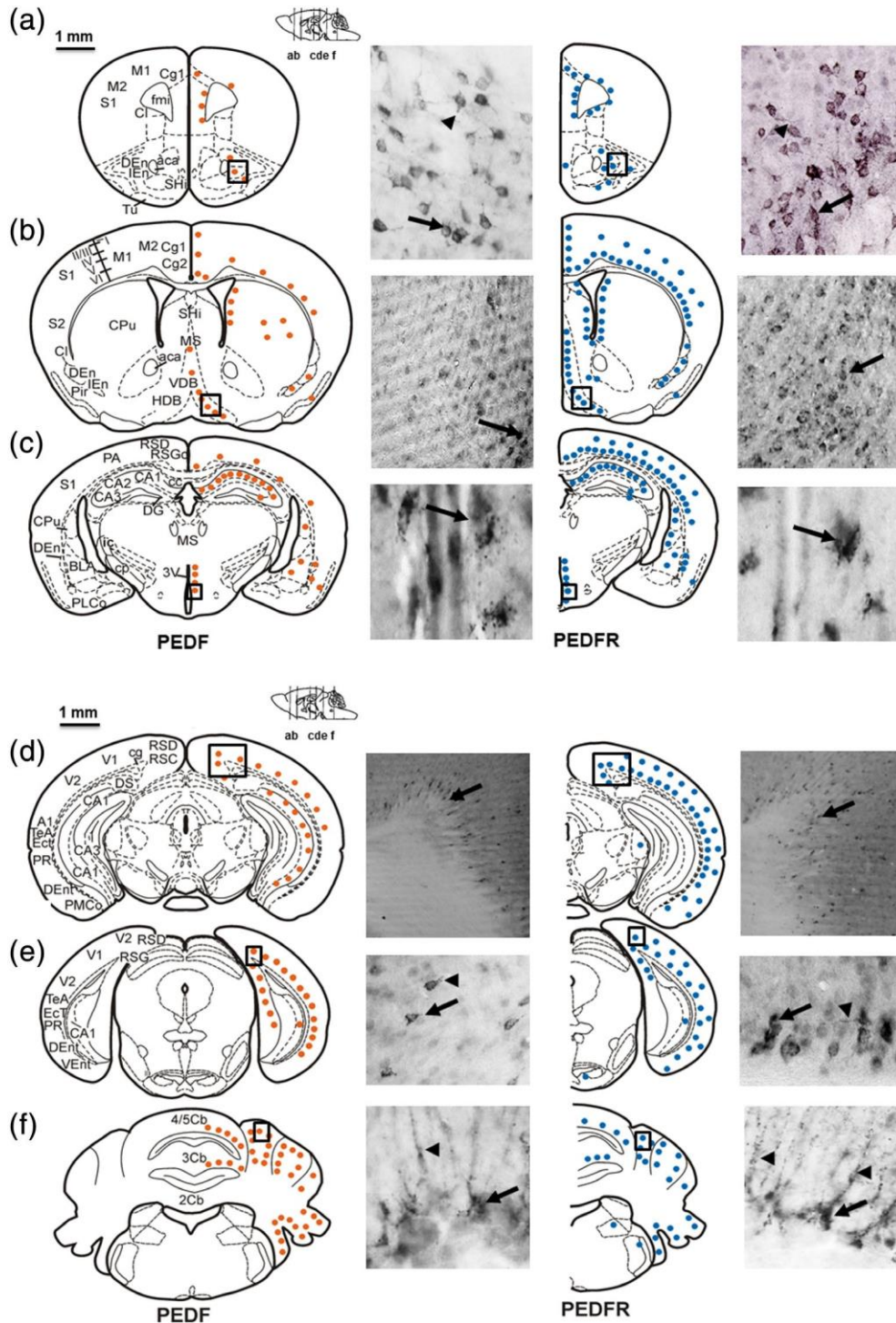
FIGURE 2 (A) A schematic drawing is depicted indicating the number of cells expressing PEDF and PEDFR in the mouse brain. Representative brain coronal sections showing the regions where PEDF (red dots on the left brain scheme) and PEDFR (blue dots on the right brain scheme) are expressed along the brain area are indicated. Cells expressing PEDF show a relatively lower signal and a difference in the number of cells than those expressing PEDFR. An equal co-distribution of positive cells is observed in the case of the hippocampus (2a–c) and periventricular zone (2A-b and 2A-c). Details of the boxes are shown at the right of each scheme. Cells are indicated with arrows and cellular processes with arrow heads. The magnifications are: 2A-a ×40, 2A-b ×20, and 2A-c ×100. Abbreviations as in Table 1. (B) A schematic drawing is depicted indicating the number of cells expressing PEDF and PEDFR in the mouse brain. Representative brain coronal sections showing the regions where PEDF (red dots on the left brain scheme) and PEDFR (blue dots on the right brain scheme) are expressed along the brain area are indicated. Cells expressing PEDF show a relatively lower signal and a difference in the number of cells than those expressing PEDFR. An equal codistribution of positive cells is observed in the cerebellum (2B-f). Details of the boxes are shown at the right of each scheme. Cells are indicated with arrows and cellular processes with arrow heads. The magnifications are: 2B-d ×10, 2B-e ×40, 2B-f ×100. Abbreviations as in Table 1

TABLE 1 Number of PEDFR and PEDF cells quantified in the different structures and its statistical significance

	2M PEDFR	2M PEDF	p value
ESTRUCTURE	Mean ± SD	Mean ± SD	
CTX-layer VI	58,007 ± 177.9	26,192 ± 35.6	0*
CTX-layer IV-V	124,580 ± 443.3	59,164 ± 199.5	0*
CTX-layer I-II-III	154,583 ± 302.5	106,121 ± 242.0	0*
Periventricular area	21,705 ± 70.5	19,112 ± 16.5	0*
CA1 HIP	19,006 ± 99.5	11,966 ± 24.9	0*
CA2-CA3 HIP	24,318 ± 82.6	9,110 ± 22.0	0*
CLAUSTRUM	10,212 ± 35.9	5,279 ± 12.0	0*
MS and DBN	7,738 ± 17.5	3,631 ± 5.3	0*
CEREB-Purk	5,014 ± 55.1	5,102 ± 5.5	2E-3*
	4/8M PEDFR	**4/8M PEDF**	
ESTRUCTURE	Mean ± SD	Mean ± SD	
CTX-layer VI	114,057 ± 148.1	31,877 ± 149.2	0*
CTX-layer IV-V	235,560 ± 557.7	119,880 ± 191.5	0*
CTX-layer I-II-III	218,564 ± 587.6	144,222 ± 756.3	0*
Periventricular area	45,658 ± 25.61	44,220 ± 10.9	0*
CA1 HIP	45,338 ± 57.7	15,251 ± 18.8	0*
CA2-CA3 HIP	49,351 ± 39.2	16,923 ± 34.4	0*
CLAUSTRUM	11,867 ± 10.3	5,994 ± 5.3	0*
MS and DBN	20,712 ± 7.7	6,556 ± 4,9	0*
CEREB-Purk	8,009 ± 21.0	8,008 ± 12.6	1.0
	12M PEDFR	**12M PEDF**	
ESTRUCTURE	Mean ± SD	Mean ± SD	
CTX-layer VI	49,911 ± 88.9	22,598 ± 177.9	0*
CTX-layer IV-V	164,481 ± 443.3	43,980 ± 88.7	0*
CTX-layer I-II-III	121,609 ± 605.0	52,767 ± 130.1	0*
Periventricular area	36,285 ± 70.5	33,052 ± 105.8	0*
CA1 HIP	13,011 ± 74.6	8,966 ± 9.9	0*
CA2-CA3 HIP	15,271 ± 13.8	9,829 ± 24.8	0*
CLAUSTRUM	7,919 ± 17.9	5,150 ± 1.8	0*
MS and DBN	5,860 ± 11.7	3,042 ± 1.2	0*
CEREB-Purk	5,014 ± 55.1	5,542 ± 31.7	0*

*Note:* Statistical significance for *$p < .05$.
Abbreviations: CEREB-Purk, purkinje layer of cerebellum; CTX-Layer I-III, Layer I, II and III of Cerebral Cortex; CTX-Layer IV-V, Layer IV and V of Cerebral Cortex; CTX-Layer VI, Layer VI of Cerebral Cortex; Layer CA1 HYP, layer CA1 of Hippocampus; Layer CA2-3 HIP, Layer Ca2 and CA3 of Hippocampus; SM and DBN, Medial Septum and Banda Diagonal Nuclei.

3.4 | Comparative distribution the PEDF and PEDFR immunoreactive cells in extratelencephalic structures

In extratelencephalic areas, the cerebellum showed cells with a strong immunostained signal for PEDF (Figures 2B-f and 8a,c, and e). Immunoreactive punctata signals were observed in pyramidal cells in the Purkinje layer, where the cell bodies are localized. Intensive positive staining was extended along the processes of these cells toward the cerebellar surface (Figures 2B-f, and 8a,c, and e). In the cerebellum, an intense signal for PEDF and PEDFR in cells was present as a positive labeling in soma, cell processes and varicosities evident in 2 month old mice and very much increased in 4–8 month old mice (Figure 8a,c for PEDF and Figure 8b,d for PEDFR), with a clear reduction in the positive signal for both pro- teins in 12 month old mice (Figure 8e,f; Table 1). In the quantifica- tion analysis, it was shown that there is a significant difference for the expression of the two proteins, the positive signal for PEDF is stronger in the 2 and 12 month old mouse groups. However, the expression was the same for both proteins in the 4–8 month old
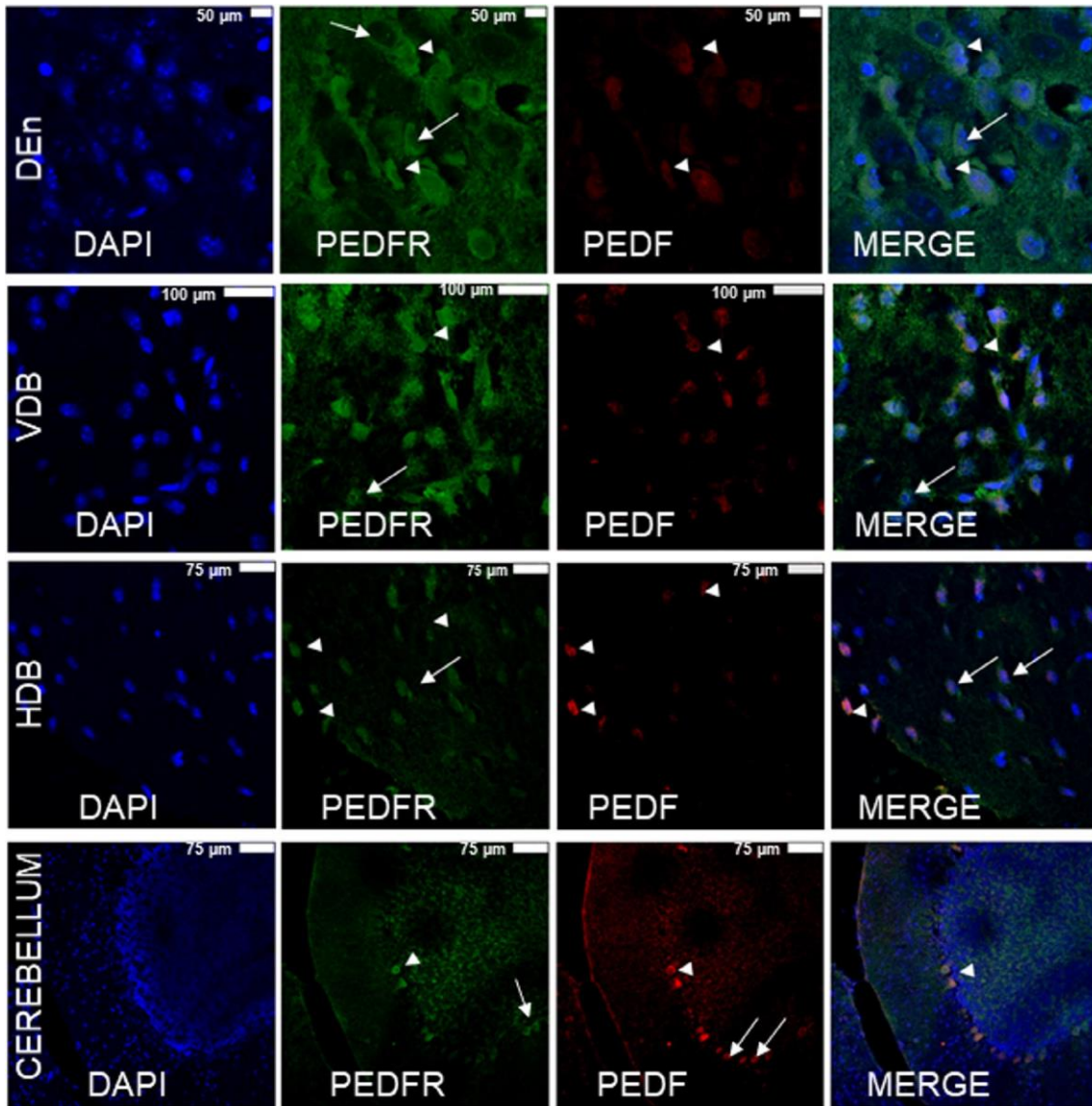
FIGURE 3 Confocal representative photomicrographs of sagittal sections showing, in the first column, in blue, the cell nuclei marked with DAPI, in the second column, in green the positive cells for anti-PNPLA2/Desnutrin/PEDFR. The third column shows the positive cells for rabbit anti-SSERPINF1/PEDF and the merge of the three is shown in the fourth column. In the first row cells of the endopiriform dorsal nucleus (DEn) are shown, in the second row nucleus of the vertical limb of the diagonal band (VDB), in the third row nucleus of the horizontal limb of the diagonal band (HDB) and in the fourth row the Purkinje layer of the cerebellum are shown. Arrows indicate single-labeled cells and arrowheads double-labeled ones

mouse groups. In the performed immunofluorescence experiments, extensive cerebellum colocalization of both proteins is shown in the purkinje layer, as well as cells expressing only PEDFR or PEDF (Figure 3).

In the periventricular and subventricular zone, a low positive signal was detected for PEDF (Figures 2A-b,c, and 9a,c, and e) and PEDFR (Figures 2A-b,c and 9 b,d, and f) in 2 month old mice, and a marked increase was observed in 4 to 8 month old mice and there were more immunolabeled cells for PEDF, however it decreased in 12-month old mice for PEDFR (Figure 9f and Table 1) and was dramatically reduced for PEDF (Figure 9e and Table 1). Only at this age, there is a considerable difference between the intensity of the labeling for both proteins, a stronger signal was detected for the PEDFR in cells of the periventricular and subventricular zone, however in the younger stages PEDF displayed a stronger signal.

Overall, PEDF and PEDFR were highly expressed in a small number of structures in the brain. Only the cerebellum, periventricular, and subventricular zone showed a strong coexistence of both pro- teins, whereas a low to moderate immunoreactivity was found in other structures such as medial septal nucleus, amygdala, or cortex (Figure 2A,B). Regarding the temporal immunodetection, remarkable differences were appreciated in PEDF and PEDFR immunostaining with aging (Figure 2A,B and Table 1).
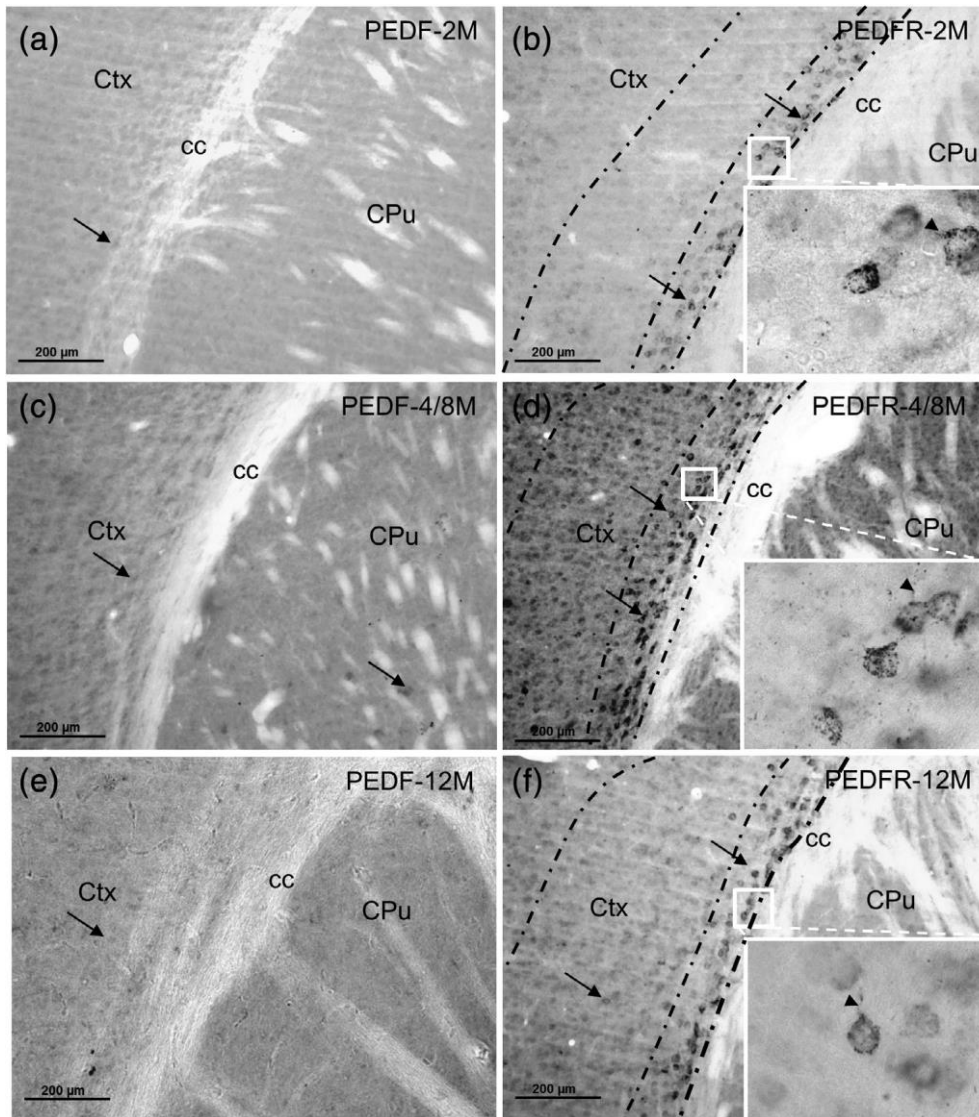
FIGURE 4 PEDF (right) and PEDFR-ir (left) immunostaining in transversal sections at different ages (2 up to 12 months). (a, c, and e) show the cross sections without positivity for PEDF staining. (b–d) sample receptor distribution localized at the different layers of the cerebral cortex, with a higher density in the layers V y VI. In (d) corresponding to 4/8 months old mice, a greater number of positive cells is observed. Details of the PEDFR-ir cells are shown in the inserts of the layer VI. a: A diffuse positive signal was mainly seen in caudate putamen. Arrow show some representative labeled cells and arrowheads show apical processes

3.5 | PEDF analysis in mouse serum and in human plasma

For the detection and quantification of PEDF in mouse serum a commercially available ELISA kit was used. A total of 22 serum samples from mice were grouped by age at different stages (2, 6, 8, and 12 months). The results showed in the young mouse (2 month old) the serum level was 155 ($SEM = 32$, 95% confidence interval [73–237]), for adult controls (6 month old) the level was 362 ng/ml ($SEM = 71$, 95% confidence interval [78–546]), for the adult controls (8 month old) the protein level was 604 ng/ml ($SEM = 111$, 95% confidence interval [317–892]), for the aged group (12 month old) the protein level was 201 nm/mL ($SEM = 17$, 95% confidence interval [155–246]).an age-dependent PEDF pres- ence in serum; the highest value for PEDF concentration was detected in 8 month old mice with a statistically significant increase ($p < .005$, $Z = -2,882$) in comparison to 2 month old mice,

whilst in the elderly mice, serum PEDF levels was dramatically reduced, statistical analysis was done by Man–Whitney U test (calculated effect size = 1,17) (Figure 10a).

To better understand the age dependent level for PEDF, plasma from human blood samples was used to measure the protein by a commercial Elisa Kit. Results indicated in the young healthy controls (2–5 years) the plasma level is 1,001 ($SEM = 0.04$, 95% confidence interval [0.89–1.11]) for adolescent healthy controls (9–15 years) the level is 2.689 ($SEM = 0.09$, 95% confidence interval [2.44–2.93]), for the adult healthy controls (18–33 years) the pro- tein level is 3.169 ($SEM = 0.07$ 95% confidence interval, [2.96–3.37]). It was found that samples from the group older than 9 years showed a significant increase in the plasma protein level ($p < .005$, $Z = -2,081$) by three times compared to the group of samples from people younger than 5 years old, statistical analysis was done by Man–Whitney U test (calculated effect size = 0,84) (Figure 10b).

FIGURE 5 PEDF (right) and PEDFR-ir (left) immunostaining in transversal sections at different ages (2 up to 12 months). (a, c, and e) show the cross sections without positivity for PEDF staining in claustrum amygdaline zone. (b, d, and f) show PEDFR-ir, a generally low signal was detected in the amygdala, except for PEDFR expression between 4 and 8 months (d). The claustrum zone showed positivity for both proteins, the expression of PEDFR being greater in all ages (b, d, and f), being more numerous between 4 and 8 months (d). BLA, basolateral amygdaloid nucleus, anterior part; BMA, basomedial amygdaloid nucleus, anterior part; Ctx, cerebral cortex; DEn, dorsal endopiriform claustrum; LA, lateral amygdaloid nucleus. Arrows indicate some labeled cells
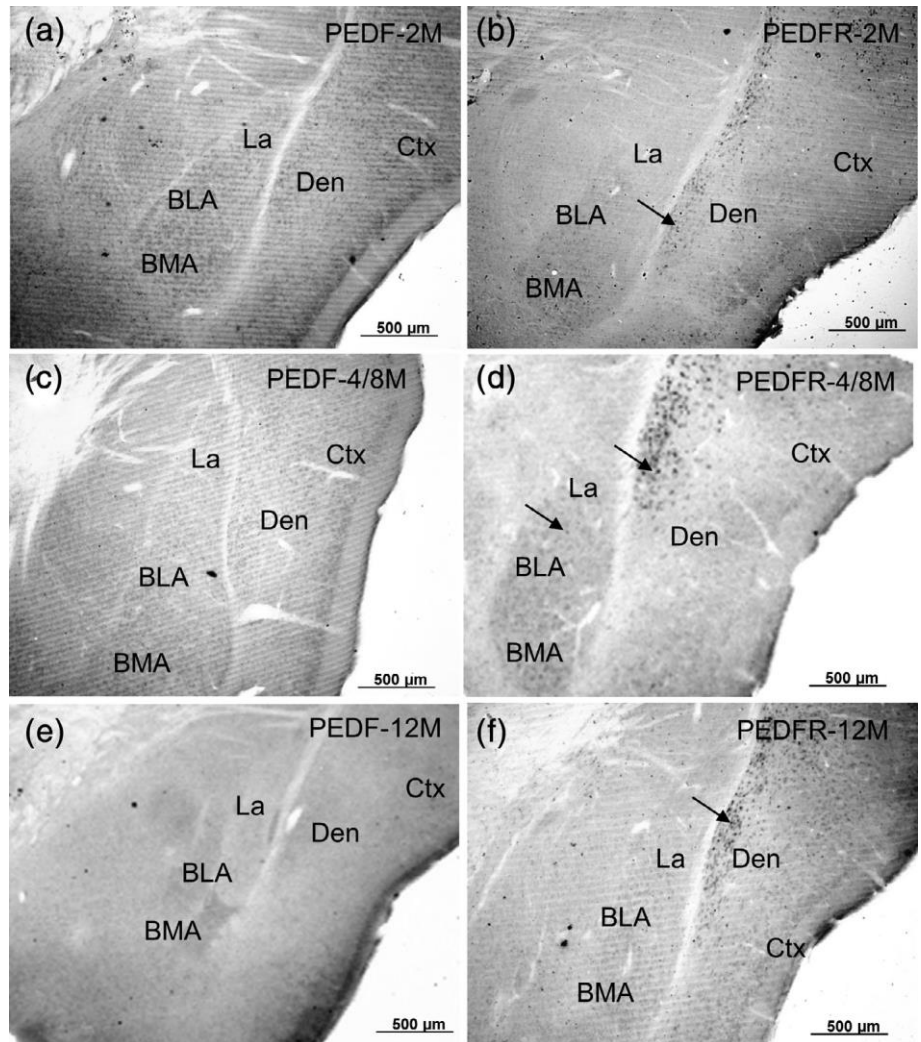
4 | DISCUSSION

The main reason to carry out this study was to perform a comprehensive characterization of PEDF protein and its receptor (PEDFR) in adult brain, since these proteins have acquired importance in the last decade due to their properties as neurotrophic and neuro- protective agents in the visual and central nervous system (Stevens, Ahmed, Vigneswara, & Ahmed, 2019). There are studies pointing to the antioxidant properties of PEDF in different biologi- cal models (Notari et al., 2006; Yamagishi et al., 2005; Yamagishi, Matsui, Nakamura, & Imaizumi, 2007; Zhang et al., 2008). Our group has an interest in antioxidant agents (de Diego-Otero et al., 2009; El Bekay et al., 2007). For this reason, a topological study of PEDF in the mouse brain becomes of high importance due to the putative protective properties of this protein. Another argument for the completion of this work is that very little has been published regarding PEDF and PEDFR expression in the cen- tral nervous system, so, a systematic immunohistochemical detec- tion of PEDF in the mouse brain may contribute to a better understanding of PEDF's role in the physiology of the CNS in further investigations.

The specificity of the PEDF antibody was previously probed by western blotting as shown by the manufacturer. A unique specific band was detected at ~50 kDa, compared with the molecular weight, as was predicted for the PEDF protein. In addition, this antibody has been extensively used on western blotting and immunofluorescence staining, found in previous published experiments carried out in mouse tissue (Haurigot et al., 2012; Hou et al., 2010).

Recently, a member of the PNPLA2 family with high affinity for PEDF and an estimated apparent molecular weight of 55 kDa has been proposed as a PEDF binding partner (Pang et al., 2007). Independent groups have identified PEDFR in other biological systems and named it iPLA2 (Jenkins et al., 2004), ATGL (Zimmermann et al., 2004), and Desnutrin (Villena, Roy, Sarkadi-Nagy, Kim, & Sul, 2004).

A previous study suggested that the binding of PEDF to PEDFR stimulates enzymatic phospholipase A (2) activity of the receptor and the subsequent releasing of bio-active fatty acids. This interaction may trigger an ulterior molecular cascade that drives to the final effect of PEDF. As for PEDF, there is no significant information regarding the expression patterns of PEDFR in adult mouse brain (Notari et al., 2006).
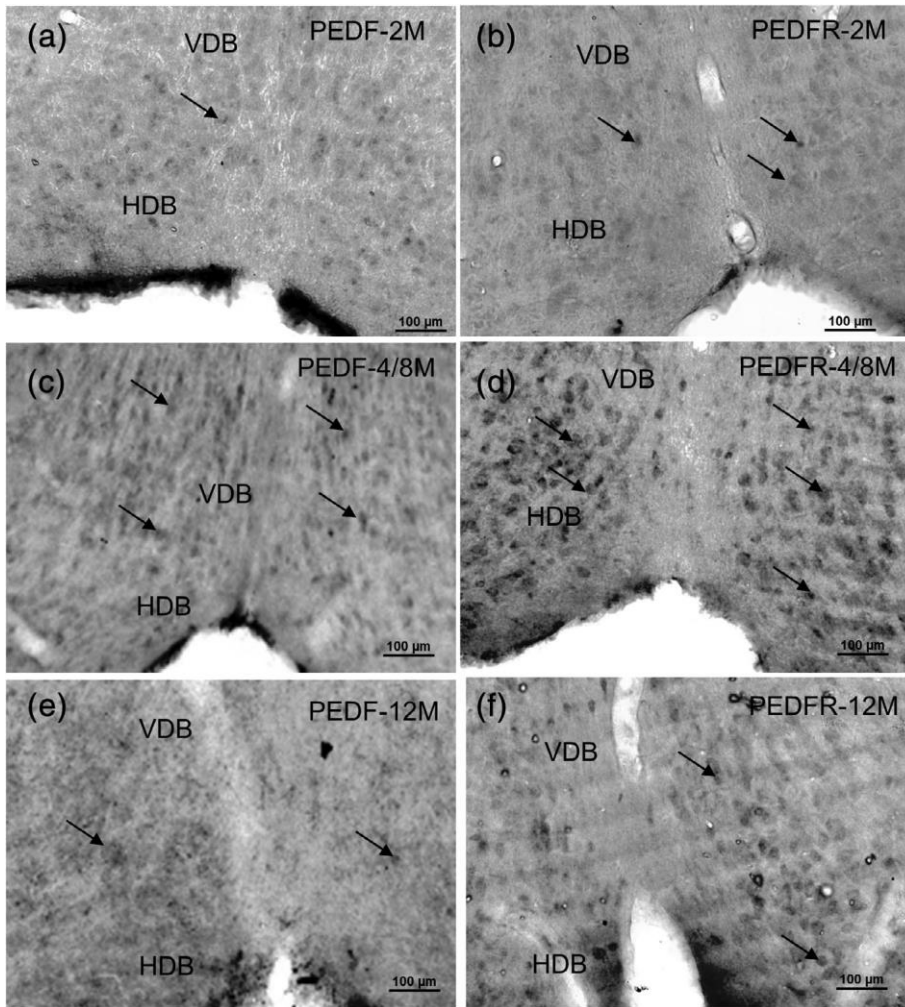
FIGURE 6 PEDF-immunoreactive (a, c, and e) and PDEFR-ir cells (b, d, and f) in transversal limb of the diagonal band sections all the studied stages (2 up to 12 months). Positive cell bodies were observed in the nucleus of the vertical limb of the diagonal band (VDB), and more laterally, in the nucleus of the horizontal limb of the diagonal band (HDB), shown for both proteins. An intense signal for PEDFR was found in all ages (b, d, and f), being more numerous between 4 and 8 months (d). Arrows indicate some labeled cells

A nonintegrin 67-kDa laminin receptor (LR) has been recently identified as another PEDF receptor (Bernard et al., 2009) which mediates PEDF angiogenesis inhibition and becomes an attractive option for treating angiogenesis-dependent diseases, such as metastatic cancer. Our work is mainly focused on the antioxidant and neurotrophic properties of PEDF, although the possibility of PEDF acting via this protein in the central nervous system is something that should not be underestimated. The results of the study indicate that the analysis of the Laminin receptor protein by western blotting showed an equal expression level in the different analyzed areas with no changes during aging.

4.1 | Cellular fraction localization of PEDF and PEDFR proteins

In view of these findings, we show for the first time, an in-depth description of the PEDFR protein in the mouse brain. The PEDFR protein was recently presented as a plasma membrane-linked protein by means of cellular fractionation. Thereby, the results that we present are in agreement with a staining pattern compatible with a clustering plasma membrane labeling for the receptor. Moreover, our

western-blots detecting the protein from homogenized mouse brain areas show an enrichment of PEDF mainly in the hippocampus, dorsal endopiriform claustrum in young adult mice, with a clear reduction of PEDF protein in the brain areas from aged mice. It is noticeable that PEDFR intensity is not showing any relevant difference in the studied areas, however, a noticeable reduction of the protein signal is observed in aged mice. Similar results indicating a reduction of both proteins are seen in the inmmunohistochemical analysis by aging. In previous reports, observations regarding subcellular localization of desnutrin/ATGL proteins (here PEDFR) were not clearly understood, as western blotting and microscopy imagines illustrated their association to membranes, but claims were made only for cytosolic proteins (Villena et al., 2004; Zimmermann et al., 2004).

4.2 | Localization of PEDF and PEDFR proteins in brain structures

Herein we used commercially available specific antibodies for the immunolabeling of PEDF and PEDFR proteins. Negative controls lacking primary antibodies were used to assure the absence of unspecific signals of the secondary antibodies (Figure S2.). We must indicate that

FIGURE 7 PEDF (right) and PEDFR (left) immunostaining in transversal hippocampus sections all the studied stages (2 up to 12 months). PEDFR expression in the hippocampus was mainly seen in the CA1 and CA3 layer of all the studied stages (2 up to 12 months). Possibility is shown for both proteins, the expression of PEDFR being greater in all ages (b, d, and f), with a peak in the labeling intensity in 4/8 month old mice for PEDFR protein (d). CA1, CA2, and CA3 correspond with CA1, CA2, and CA3 fields of hippocampus
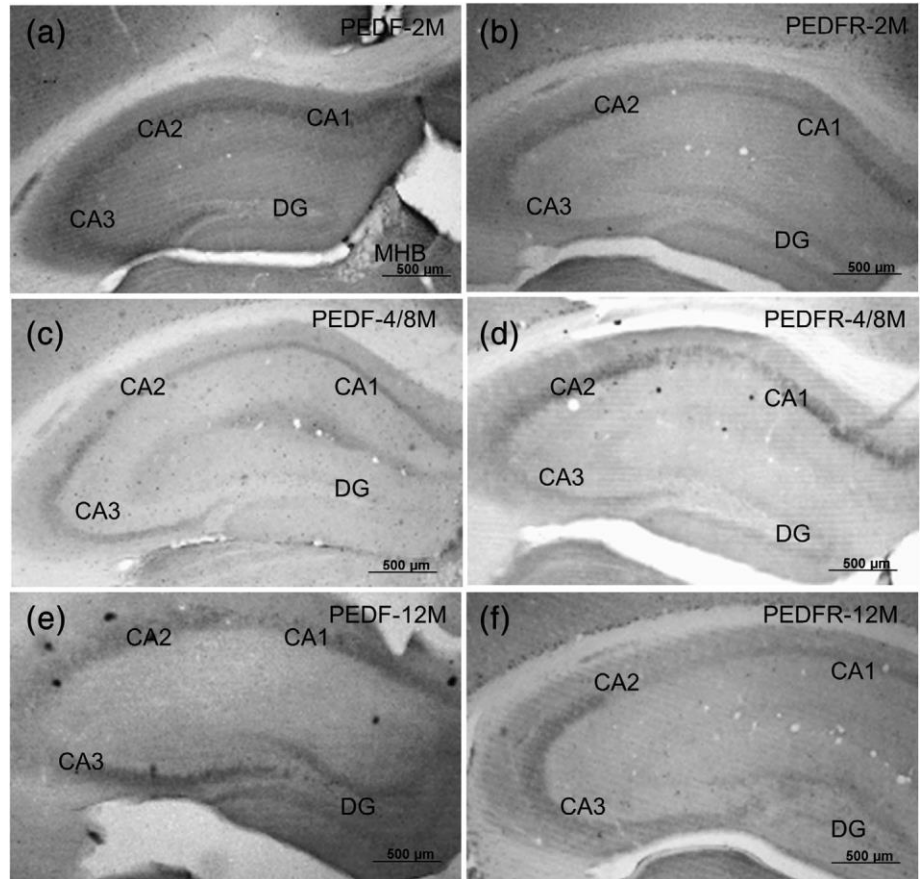
we had some difficulty in the immunolabeling of both proteins due in part to its low expression in brain and also by the poor amount of previous methodological references. Brains from mice of different ages (2–12 months) were analyzed and changes in PEDF and PEDFR levels were found with aging. In general, the concomitant expression of both proteins was strong only in few areas in the brain such as hippocampus, cerebellum or subventricular areas.

PEDF showed a cytoplasmic staining pattern in the molecular layer of the cerebellum, as it has been previously reported in other works (Sanagi, Yabe, & Yamada, 2007). Sanagi and collaborators described that the PEDF protein and mRNA were mostly confined and co-localized within calbindin-positive cells in the Purkinje cell layer and that the kainic acid-induced cerebellum injury stimulated PEDF expression in GFAP-positive reactive astrocytes (Sanagi et al., 2007).

PEDFR expression in brain is not only restricted to the cerebellum and septal nuclei but also in other telencephalic and extratelencephalic structures. The most striking staining pattern was found in the cortex, where the deepest layer of cells was heavily labeled. When comparing the expression of PEDF and PEDFR we noticed that only the molecular layer in the cerebellum, the CA1-CA2-CA3 of the hippocampus and the subventricular zone show elevated expression and codistribution of both proteins. It has to be taken into account that PEDF is a soluble protein and that PEDFR is localized in the cellular membrane, and therefore, codistribution is not

hard to miss in certain PEDFR-expressing structures. Furthermore, the physiological function of the PEDF/PEDFR partnership is still unclear in the brain. Although the expression of PEDF in cerebellum and glial cells have been reported in previous investigations (Sanagi et al., 2007), expression studies in neurons, glia of the brain areas need to be carried out in the future, to further analyze the relevance of this protein for cellular brain survival and physiology.

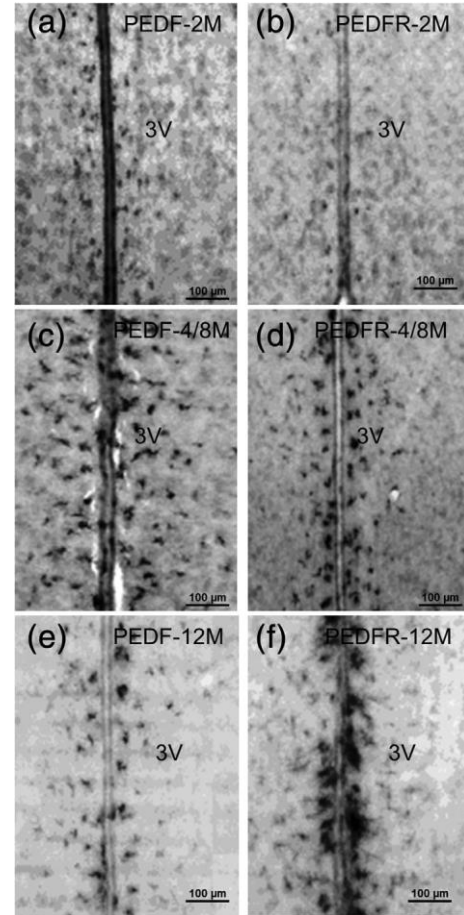## 4.3 | Codistriburion of PEDF and PEDFR in brain areas

Our findings indicate the concomitant presence of PEDF and PEDFR in the subventricular zone of the third ventricle, showing an intense labeling at 4 and 6 months. There are no previous studies describing the expression of both proteins in the same areas. Moreover, this is the first report showing PEDF being present in structures related with the limbic system. Positive cells for both PEDF and PEDFR were seen in CA1 and CA3 layers of the hippocampus, the diagonal band and in the medial septal nucleus. It is known that the septal nuclei play a role in reward and reinforcement along with the nucleus accumbens (where we also found expression of the PEDFR protein). The septal nuclei are in part an evolutionary and developmental outgrowth of the hippocampus and the hypothalamus, serving as a linkage between hippocampus, hypothalamus, and brainstem (Risold & Swanson, 1996;
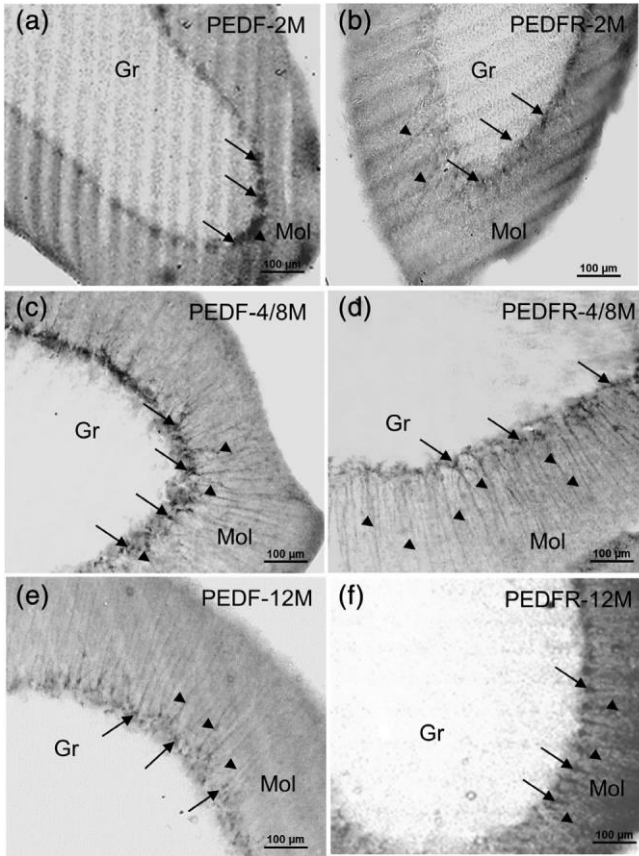
FIGURE 8 PEDF (right side panel) and PEDFR (left side panel) immunostaining in transversal sections in cerebellum of all the studied stages (2 up to 12 months). (a) Show positive cells in the Purkinje layer from which processes are projected toward the molecular layer. (a, b) Sections corresponding to mice of 2 months of age, with scarce positive signal. (c, d) The most intense positive signal in mice of 4/8 months. (e,f) Slight decrease after 12 months for PEDF. Arrow show some representative labeled Purkinje cells and arrowheads show some processes. Gr, granular layer (cerebellum); Mol, molecular layer (cerebellum)

FIGURE 9 PEDF (right side panel) and PEDFR-ir (left side panel) immunostaining in transversal sections in ventricles. (a, b) less intense in mice of 2 months. Higher number of positive cells show the ages between 4 and 8 (c, d) months decreasing again for PEDF in 12-month-old mice (e, f), the number of positive cells was higher in the cells expressing PEDFR. 3V: third ventricle

Swanson & Cowan, 1979). Therefore, the way in which PEDF could be involved in the physiology of the hippocampus-hypothalamus pathway is something that remains unclear and that deserves further studies. Recent findings indicate that PEDF contributes to dendritic growth and Wnt signaling activation in the hippocampus of adult mice, and the involvement of PEDF and its related mechanism in depression with proposed therapeutically effects was proposed (Tian et al., 2019).

This work shows that both PEDF and PEDFR are also found in brain structures, such as the cerebellum, hippocampus, and subventricular area. However, our studies of these two proteins, using confocal microscopy identify positive signal in specific cellular types such as the cerebellar Purkinje cells that show colocalization for both proteins in several cells whilst other cells showed only one type of these two proteins. Similar results were found in endopiriform dorsal nucleus (DEn) and also in the vertical limb of the diagonal band (VDB) or the horizontal limb of the diagonal band (HDB). In this regard, even

though the cerebellum is a structure that has been typically related with the motor-related tasks, new findings in the field have revealed that it is also involved in cognitive roles such as attention and language, and probably in emotional functions like the regulation of fear and pleasure responses (Doya, 2000; Wolf, Rapoport, & Schweizer, 2009). Furthermore, it is known that the subventricular zone is a known site of neurogenesis and self-renewing neurons in the adult brain (Lim & Alvarez-Buylla, 1999), allowing for the interaction between different cell types and also as extracellular molecules promoting cellular proliferation. There are references indicating that PEDF is secreted by components of the murine subventricular zone and promotes self-renewal of adult NSCs in vitro (Ramírez-Castillejo et al., 2006). Our results are in agreement with the existence of PEDF-positive cells in this area and, in addition, the data provided in this work shows that PEDFR is also expressed in the same region. Taken together, these facts suggest that PEDF is a niche-derived reg- ulator of adult NSCs and further analysis are deserved to deeply understand the relation. Nevertheless, PEDF functions are somehow
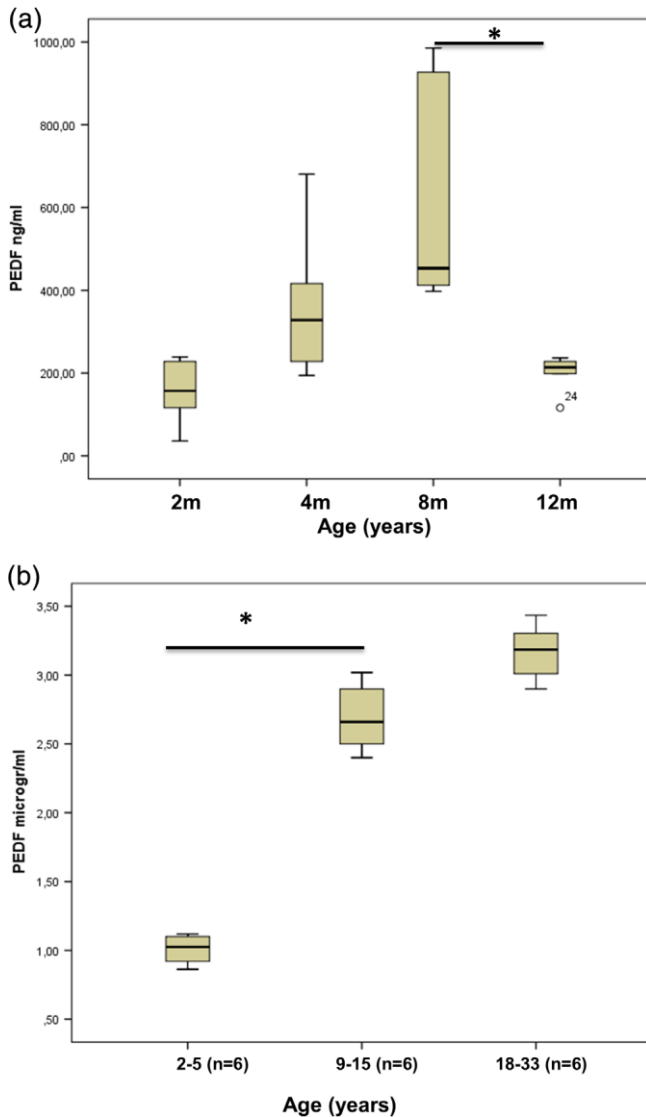
FIGURE 10 PEDF in mouse serum (a) and human plasma (b). PEDF was detected in serum from mice and human plasma of different ages with the ELISA method. Results show age-dependent PEDF levels with a clear reduction during aging. Data are mean ± *SEM* of 5–6 mice for group. * represents $p < .01$ versus the respective group by U Mann–Whitney test [Color figure can be viewed at wileyonlinelibrary.com]

involved in areas where the modulation during aging might have a great impact on cognitive and emotional components.

It is worth to say that PEDF has important roles in the control of numerous pathologies like cancer (Baxter-Holland & Dass, 2018; Broadhead & Dass, 2009; Hoshina et al., 2010; Manalo, Choong, Becerra, & Dass, 2011) but not much data have been published about the functions of PEDF in neurodevelopmental impairments and how in pathological conditions the expression of PEDF and PEDFR in the brain could be altered. In recent years, our group has been investigating the pathophysiology of neurodevelopmental disorders and autism where the presence of an elevated production of free radicals has been demonstrated (de Diego-Otero et al., 2009; El Bekay et al., 2007). There is experimental evidence that link Purkinje cell dysfunctions with the

presence of autism (Bauman & Kemper, 2005; Bedogni et al., 2010) and PEDF showed an intense positive signal most probably in Purkinje cells. Further studies must be done to understand the possible functions of both proteins during developmental stages.

4.4 | PEDF detection in serum

In order to reinforce the idea of a modulation of PEDF level by age, we performed an ELISA technique to measure PEDF in serum from mice of different ages. The results have shown a significant increase of the PEDF protein concentration in 8 month-old mice. It is worth noting that this research also detected an increase in PEDF immune-detection by immunohistochemistry in middle-aged mice. The PEDF measurement in human plasma demonstrated an age-related variation in PEDF levels as higher levels occur in the samples from control people over 9 years old.

The present work reported the existence of an age-related modulation of PEDF levels in blood with a maximum of PEDF detection in adults. Not much data on this regard are found in the bibliography. One work indicates an increased expression level of PEDF within aged mesenchymal stem cells (Liang et al., 2013) and the majority of published works are focused on the modulation of PEDF levels in pathological conditions (Arimura et al., 2011; Chen, Fan, Huang, Xu, & Zhang, 2012; Tahara et al., 2011).

The most recent publication suggested that PEDF-mediated neuroprotection against oxidant injury is largely mediated via ERK1/2 and Bcl-2, indicating that PEDF preserves the viability of oxidative challenged neurons (Sanchez et al., 2011), and may be related to the inhibition of NADPH oxidase-mediated oxidative stress (Maeda, Matsui, Takeuchi, & Yamagishi, 2011).

It has been recently proposed that null mutations of the PEDF gene results in Osteogenesis Imperfecta Type VI, a rare autosomal recessive bone disease characterized by multiple fractures, highlighting a critical developmental function for this protein. Therefore, PEDF affects various stem cell populations in the development of bone, brain, muscle, and eye (Sagheer, Gong, & Chung, 2015). PEDF, which promotes survival of retinal ganglion cells through STAT3 activation by PEDFR dependent signaling could be useful in neurodegenerative disorders (Eichler et al., 2017; Huang et al., 2018).

All these facts lead us to highlight the importance of an exhaustive investigation on the modulation of the expression of PEDF and PEDFR in the central nervous system, suggesting a physiological role in specific brain areas and also relating to aging processes. All these studies lead to new challenges to study neurological and psychiatric disorders where oxidative stress is present, to address future studies devoted to developing new therapeutic interventions.

5 | CONCLUSIONS

In conclusion, our findings show that first, both PEDF and PEDFR were present in different areas of the mouse brain with a particular signaling

pattern for each protein, second, codistribution of both proteins, detected by an intense labeling, was restricted to few structures, principally related to the limbic system (hippocampus), subventricular zone and cerebellum. Third, and age dependent level of both proteins has been found in the brain areas and in human and mouse blood.

COMPETING INTERESTS

The authors declare that they have no competing interests.

AUTHOR CONTRIBUTIONS

Rosa María Giráldez-Pérez, Yolanda de Diego-Otero, Lucía Pérez Costillas, and Raúl Heredia-Farfan participated in the design of the study, carried out part of the immunohistochemical and ELISA assays and drafted the manuscript. Elena Lima-Cabello performed part of the western blots shown in the present article. Rosa María Giráldez-Pérez performed cell quantification and statistical analysis. Lourdes Sanchez-Salido helped in some of the immunohistochemical procedures and in the maintenance and perfusion of the animals. Yolanda de Diego-Otero, Rocío Calvo Medina, and Lucía Pérez Costillas performed the statistical analysis. All authors read and approved the final manuscript.

DATA AVAILABILITY STATEMENT

The data that support the findings of this study are available from the corresponding author upon reasonable request.

ORCID

Yolanda de Diego-Otero https://orcid.org/0000-0003-2384-8349

REFERENCES

Alberdi, E., Aymerich, M. S., & Becerra, S. P. (1999). Binding of pigment epithelium-derived factor (PEDF) to retinoblastoma cells and cerebellar granule neurons. Evidence for a PEDF receptor. *The Journal of Biological Chemistry*, *274*, 31605–31612.

Amaral, J., & Becerra, S. P. (2010). Effects of human recombinant PEDF protein and PEDF-derived peptide 34-mer on choroidal neovascularization. *Investigative Ophthalmology & Visual Science*, *51*, 1318–1326. https://doi.org/10.1167/iovs.09-4455

Andreu-Agulló, C., Morante-Redolat, J. M., Delgado, A. C., & Fariñas, I. (2009). Vascular niche factor PEDF modulates notch-dependent stemness in the adult subependymal zone. *Nature Neuroscience*, *12*, 1514–1523. https://doi.org/10.1038/nn.2437

Araki, T., Taniwaki, T., Becerra, S. P., Chader, G. J., & Schwartz, J. P. (1998). Pigment epithelium-derived factor (PEDF) differentially protects immature but not mature cerebellar granule cells against apoptotic cell death. *Journal of Neuroscience Research*, *53*, 7–15. https://doi.org/10.1002/(SICI)1097-4547(19980701)53:1<7::AID-JNR2>3.0.CO;2-F

Arimura, T., Miura, S., Sugihara, M., Iwata, A., Yamagishi, S., & Saku, K. (2011). Association between plasma levels of pigment epithelium-derived factor and renal dysfunction in patients with coronary artery disease. *Cardiology Journal*, *18*, 515–520.

Barnstable, C. J., & Tombran-Tink, J. (2004). Neuroprotective and anti-angiogenic actions of PEDF in the eye: Molecular targets and therapeutic potential. *Progress in Retinal and Eye Research*, *23*, 561–577. https://doi.org/10.1016/j.preteyeres.2004.05.002

Bauman, M. L., & Kemper, T. L. (2005). Neuroanatomic observations of the brain in autism: A review and future directions. *International Journal of Developmental Neuroscience*, *23*, 183–187. https://doi.org/10.1016/j.ijdevneu.2004.09.006

Baxter-Holland, M., & Dass, C. R. (2018). Pigment epithelium-derived factor: A key mediator in bone homeostasis and potential for bone regenerative therapy. *The Journal of Pharmacy and Pharmacology*, *70*, 1127–1138. https://doi.org/10.1111/jphp.12942

Becerra, S. P., Fariss, R. N., Wu, Y. Q., Montuenga, L. M., Wong, P., & Pfeffer, B. A. (2004). Pigment epithelium-derived factor in the monkey retinal pigment epithelium and interphotoreceptor matrix: Apical secretion and distribution. *Experimental Eye Research*, *78*, 223–234.

Bedogni, F., Hodge, R. D., Nelson, B. R., Frederick, E. A., Shiba, N., Daza, R. A., & Hevner, R. F. (2010). Autism susceptibility candidate 2 (Auts2) encodes a nuclear protein expressed in developing brain regions implicated in autism neuropathology. *Gene Expression Patterns*, *10*, 9–15. https://doi.org/10.1016/j.gep.2009.11.005

Bernard, A., Gao-Li, J., Franco, C. A., Bouceba, T., Huet, A., & Li Z. (2009). Laminin receptor involvement in the anti-angiogenic activity of pigment epithelium-derived factor. *The Journal of Biological Chemistry*, *284*, 10480–10490. https://doi.org/10.1074/jbc.M809259200

Bilak, M. M., Corse, A. M., Bilak, S. R., Lehar, M., Tombran-Tink, J., & Kuncl, R. W. (1999). Pigment epithelium-derived factor (PEDF) protects motor neurons from chronic glutamate-mediated neurodegeneration. *Journal of Neuropathology and Experimental Neurology*, *58*, 719–728.

Blasco, B., Avendaño, C., & Cavada, C. (1999). A stereological analysis of the lateral geniculate nucleus in adult Macaca nemestrina monkeys. *Vis Neurosci*, *16*, 933–941.

Bouck, N. (2002). PEDF: Anti-angiogenic guardian of ocular function. *Trends in Molecular Medicine*, *2002*(8), 330–334.

Broadhead, M. L., Dass, C. R., & Choong, P. F. (2009). In vitro and in vivo biological activity of PEDF against a range of tumors. *Expert Opinion on Therapeutic Targets*, *13*, 1429–1438. https://doi.org/10.1517/14728220903307475

Castaño, E. M., Roher, A. E., Esh, C. L., Kokjohn, T. A., & Beach, T. (2006). Comparative proteomics of cerebrospinal fluid in neuropathologically-confirmed Alzheimer's disease and non-demented elderly subjects. *Neurological Research*, *28*, 155–163. https://doi.org/10.1179/016164106X98035

Cayouette, M., Smith, S. B., Becerra, S. P., & Gravel, C. (1999). Pigment epithelium-derived factor delays the death of photoreceptors in mouse models of inherited retinal degenerations. *Neurobiology of Disease*, *6*, 523–532. https://doi.org/10.1006/nbdi.1999.0263

Chen, L., Fan, R., Huang, X., Xu, H., & Zhang, X. (2012). Reduced levels of serum pigment epithelium-derived factor in women with endometriosis. *Reproductive Sciences*, *19*, 64–69. https://doi.org/10.1177/1933719111413300

Crawford, S. E., Stellmach, V., Ranalli, M., Huang, X., Huang, L., Volpert, O., … Bouck, N. (2001). Pigment epithelium-derived factor (PEDF) in neuroblastoma: A multifunctional mediator of Schwann cell antitumor activity. *Journal of Cell Science*, *114*, 4421–4428.

Dawson, D. W., Volpert, O. V., Gillis, P., Crawford, S. E., Xu, H., Benedict, W., & Bouck, N. P. (1999). Pigment epithelium-derived fac- tor: A potent inhibitor of angiogenesis. *Science*, *285*, 245–248.

de Diego-Otero, Y., Romero-Zerbo, Y., El Bekay, R., Decara, J., Sanchez, L., Rodriguez-de, F. F., & del Arco-Herrera, I. (2009). Alpha-tocopherol protects against oxidative stress in the fragile X knockout mouse: An experimental therapeutic approach for the Fmr1 deficiency. *Neuropsychopharmacology*, *34*, 1011–1026. https://doi.org/10.1038/npp.2008.152

DeCoster, M. A., Schabelman, E., Tombran-Tink, J., & Bazan, N. G. (1999). Neuroprotection by pigment epithelial-derived factor against gluta- mate toxicity in developing primary hippocampal neurons. *Journal of Neuroscience Research*, *56*, 604–610. https://doi.org/10.1002/(SICI)1097-4547(19990615)56:6<604::AID-JNR6>3.0.CO;2-B

Doll, J. A., Stellmach, V. M., Bouck, N. P., Bergh, A. R., Lee, C., Abramson, L. P., … Crawford, S. E. (2003). Pigment epithelium-derived factor regulates the vasculature and mass of the prostate and pan- creas. *Nature Medicine*, *9*, 774–780. https://doi.org/10.1038/nm870

Doya, K. (2000). Complementary roles of basal ganglia and cerebellum in learning and motor control. *Current Opinion in Neurobiology*, *10*, 732–739.

Eichler, W., Savkoviₗc-Cvijiₗc, H., Bürger, S., Beck, M., Schmidt, M., Wiedemann, P., … Unterlauft, J. D. (2017). Müller cell-derived PEDF mediates neuroprotection via STAT3 activation. *Cellular Physiology and Biochemistry*, *44*, 1411–1424. https://doi.org/10.1159/000485537

El Bekay, R., Romero-Zerbo, Y., Decara, J., Sanchez-Salido, L., Del Arco-Herrera, I., Rodríguez-de, F. F., & de Diego-Otero, Y. (2007). Enhanced markers of oxidative stress, altered antioxidants and NADPH-oxidase activation in brains from fragile X mental retardation 1-deficient mice, a pathological model for fragile X syndrome. *The European Journal of Neuroscience*, *26*, 3169–3180. https://doi.org/10.1111/j.1460-9568.2007.05939.x

Franklin, K. B. J., & Paxinos, G. (2007). *The mouse brain in stereotaxic coordinates* (3rd ed.). San Diego: Academic Press.

Garcia, M., Fernandez-Garcia, N. I., Rivas, V., Carretero, M., Escamez, M. J., Gonzalez-Martin, A., … Del Rio, M. (2004). Inhibition of xenografted human melanoma growth and prevention of metastasis development by dual antiangiogenic/antitumor activities of pigment epithelium-derived factor. *Cancer Research*, *64*, 5632–5642. https://doi.org/10.1158/0008-5472.CAN-04-0230

Gettins, P. G., Simonovic, M., & Volz, K. (2002). Pigment epithelium-derived factor (PEDF), a serpin with potent anti-angiogenic and neurite outgrowth-promoting properties. *Biological Chemistry*, *383*, 1677–1682. https://doi.org/10.1515/BC.2002.188

Giráldez-Pérez, R. M., Avila, M. N., Feijóo-Cuaresma, M., Heredia, R., De Diego-Otero, Y., Real, M. A., & Guirado, S. (2013). Males but not females show differences in calbindin immunoreactivity in the dorsal thalamus of the mouse model of fragile X syndrome. *The Journal of Comparative Neurology*, *521*, 894–911.

Gundersen, H. J., Bagger, P., Brendtsen, T. F., Evans, S. M., Korbo, L., Marcussen, L., … Pakkenberg, B. (1988). The new stereological tools: Disector, fractionator, nucleator and point sampled intercepts and their use in pathological research and diagnosis. *AMPIS*, *96*, 857–881.

Haurigot, V., Villacampa, P., Ribera, A., Bosch, A., Ramos, D., Ruberte, J., & Bosch, F. (2012). Long-term retinal PEDF overexpression prevents neovascularization in a murine adult model of retinopathy. *PLoS ONE*, *7*, e41511. https://doi.org/10.1371/journal.pone.0041511

Hoshina, D., Abe, R., Yamagishi, S. I., & Shimizu, H. (2010). The role of PEDF in tumor growth and metastasis. *Current Molecular Medicine*, *10*, 292–295.

Hou, H. Y., Liang, H. L., Wang, Y. S., Zhang, Z. X., Wang, B. R., Shi, Y. Y., … Cai, Y. (2010). A therapeutic strategy for choroidal neovascularization based on recruitment of mesenchymal stem cells to the sites of lesions. *Molecular Therapy*, *18*, 1837–1845. https://doi.org/10.1038/mt.2010.144

Houenou, L. J., D'Costa, A. P., Li, L., Turgeon, V. L., Enyadike, C., Alberdi, E., & Becerra, S. P. (1999). Pigment epithelium-derived factor promotes the survival and differentiation of developing spinal motor neurons. *The Journal of Comparative Neurology*, *412*, 506–514.

Huang, M., Qi, W., Fang, S., Jiang, P., Yang, C., Mo, Y., … Gao, G. (2018). Pigment epithelium-derived factor plays a role in Alzheimer's disease by negatively regulating Aβ42. *Neurotherapeutics*, *15*, 728–741. https://doi.org/10.1007/s13311-018-0628-1

Jenkins, C. M., Mancuso, D. J., Yan, W., Sims, H. F., Gibson, B., & Gross, R. W. (2004). Identification, cloning, expression, and purification of three novel human calcium-independent phospholipase A2 family members possessing triacylglycerol lipase and acylglycerol trans- acylase activities. *The Journal of Biological Chemistry*, *279*, 48968–48975. https://doi.org/10.1074/jbc.M407841200

Kuncl, R. W., Bilak, M. M., Bilak, S. R., Corse, A. M., Royal, W., & Becerra, S. P. (2002). Pigment epithelium-derived factor is elevated in CSF of patients with amyotrophic lateral sclerosis. *Journal of Neuro- chemistry*, *81*, 178–184.

Liang, H., Hou, H., Yi, W., Yang, G., Gu, C., Lau, W. B., … Yi, D. (2013). Increased expression of pigment epithelium-derived factor in aged mesenchymal stem cells impairs their therapeutic efficacy for attenu- ating myocardial infarction injury. *European Heart Journal*, *34*, 1681–1690. https://doi.org/10.1093/eurheartj/ehr131

Lim, D. A., & Alvarez-Buylla, A. (1999). Interaction between astrocytes and adult subventricular zone precursors stimulates neurogenesis. *Proceedings of the National Academy of Sciences of the United States of America*, *96*, 7526–7531.

Maeda, S., Matsui, T., Takeuchi, M., & Yamagishi, S. (2011). Pigment epithelium-derived factor (PEDF) blocks advanced glycation end prod- ucts (AGEs)-RAGE-induced suppression of adiponectin mRNA level in adipocytes by inhibiting NADPH oxidase-mediated oxidative stress generation. *International Journal of Cardiology*, *152*, 408–410. https://doi.org/10.1016/j.ijcard.2011.08.043

Manalo, K. B., Choong, P. F., Becerra, S. P., & Dass, C. R. (2011). Pigment epithelium-derived factor as an anticancer drug and new treatment methods following the discovery of its receptors: A patent perspec- tive. *Expert Opinion on Therapeutic Patents*, *21*, 121–130. https://doi.org/10.1517/13543776.2011.545347

Moreno-Navarrete, J. M., Touskova, V., Sabater, M., Mraz, M., Drapalova, J., Ortega, F., … Fernández-Real, J. M. (2013). Liver, but not adipose tissue PEDF gene expression is associated with insulin resis- tance. *International Journal of Obesity*, *37*, 1230–1237. https://doi.org/10.1038/ijo.2012.223

Notari, L., Baladron, V., Aroca-Aguilar, J. D., Balko, N., Heredia, R., Meyer, C., … Becerra, S. P. (2006). Identification of a lipase-linked cell membrane receptor for pigment epithelium-derived factor. *The Journal of Biological Chemistry*, *281*, 38022–38037. https://doi.org/10.1074/jbc.M600353200

Pang, I. H., Zeng, H., Fleenor, D. L., & Clark, A. F. (2007). Pigment epithelium-derived factor protects retinal ganglion cells. *BMC Neuro- science*, *8*, 11. https://doi.org/10.1186/1471-2202-8-11

Perez-Mediavilla, L. A., Chew, C., Campochiaro, P. A., Nickells, R. W., Notario, V., Zack, D. J., & Becerra, S. P. (1998). Sequence and expres- sion analysis of bovine pigment epithelium-derived factor. *Biochimica et Biophysica Acta*, *1398*, 203–214.

Ramírez-Castillejo, C., Sánchez-Sánchez, F., Andreu-Agulló, C., Ferrón, S. R., Aroca-Aguilar, J. D., Sánchez, P., … Fariñas, I. (2006). Pigment epithelium-derived factor is a niche signal for neural stem cell renewal. *Nature Neuroscience*, *9*, 331–339. https://doi.org/10.1038/nn1657

Risold, P. Y., & Swanson, L. W. (1996). Structural evidence for functional domains in the rat hippocampus. *Science*, *272*, 1484–1486.

Sagheer, U., Gong, J., & Chung, C. (2015). Pigment epithelium-derived fac- tor (PEDF) is a determinant of stem cell fate: Lessons from an ultra- rare disease. *Journal of Developmental Biology*, *3*, 112–128. https://doi.org/10.3390/jdb3040112

Sanagi, T., Yabe, T., & Yamada, H. (2007). Changes in pigment epithelium- lesion in rat. *Neuroscience Letters*, *424*, 66–71. https://doi.org/10. 1016/j.neulet.2007.07.021

Sanchez, A., Tripathy, D., Yin, X., Luo, J., Martinez, J., & Grammas, P. (2011). Pigment epithelium-derived factor (PEDF) protects cortical neurons in vitro from oxidant injury by activation of extracellular signal-regulated kinase (ERK) 1/2 and induction of Bcl-2. *Neuroscience Research*, *72*, 1–8. https://doi.org/10.1016/j.neures.2011.09.003

Sterio, D. C. (1984). The unbiased estimation of number and sizes of arbi- trary particles using the disector. *Journal of Microscopy*, *134*, 127–136. Stevens, A. R., Ahmed, U., Vigneswara, V., & Ahmed, Z. (2019). Pigment epithelium-derived factor promotes axon regeneration and functional recovery after spinal cord injury. *Molecular Neurobiology*, *56*, 7490–7507.

Storozheva, Z. I., Proshin, A. T., Zhokhov, S. S., Sherstnev, V. V., Rodionov, I. L., Lipkin, V. M., & Kostanyan, I. A. (2006). Hexapeptides HLDF-6 and PEDF-6 restore memory in rats after chronic intracerebroventricular treatment with beta-amyloid peptide Abeta (25-35). *Bulletin of Experimental Biology and Medicine*, *141*, 319–322.

Subramanian, P., Notario, P. M., & Becerra, S. P. (2010). Pigment epithelium-derived factor receptor (PEDF-R): A plasma membrane- linked phospholipase with PEDF binding affinity. *Advances in Experi- mental Medicine and Biology*, *664*, 29–37. https://doi.org/10.1007/ 978-1-4419-1399-9_4

Sugita, Y., Becerra, S. P., Chader, G. J., & Schwartz, J. P. (1997). Pigment epithelium-derived factor (PEDF) has direct effects on the metabolism and proliferation of microglia and indirect effects on astrocytes. *Jour- nal of Neuroscience Research*, *49*, 710–718. https://doi.org/10.1002/(SICI)1097-4547(19970915)49:6<710::AID-JNR5>3.0.CO;2-A

Swanson, L. W., & Cowan, W. M. (1979). The connections of the septal region in the rat. *The Journal of Comparative Neurology*, *186*, 621–655. https://doi.org/10.1002/cne.901860408

Tahara, N., Yamagishi, S., Tahara, A., Nitta, Y., Kodama, N., Mizoguchi, M., … Imaizumi, T. (2011). Serum level of pigment epithelium-derived fac- tor is a marker of atherosclerosis in humans. *Atherosclerosis*, *219*, 311–315. https://doi.org/10.1016/j.atherosclerosis.2011.06.022

Taniwaki, T., Hirashima, N., Becerra, S. P., Chader, G. J., Etcheberrigaray, R., & Schwartz, J. P. (1997). Pigment epithelium- derived factor protects cultured cerebellar granule cells against glutamate-induced neurotoxicity. *Journal of Neurochemistry*, *68*, 26–32.

Tian, T., Yang, Y., Xu, B., Qin, Y., Zang, G., Zhou, C., … Xie, P. (2019). Pig- ment epithelium-derived factor alleviates depressive- like behaviors in mice by modulating adult hippocampal synaptic growth and Wnt path- way. *Progress in Neuro-Psychopharmacology & Biological Psychiatry*, *98*, 109792.

Tombran-Tink, J., Chader, G. G., & Johnson, L. V. (1991). PEDF: A pigment epithelium-derived factor with potent neuronal differentiative activity. *Experimental Eye Research*, *53*, 411–414.

Villena, J. A., Roy, S., Sarkadi-Nagy, E., Kim, K. H., & Sul, H. S. (2004). Desnutrin, an adipocyte gene encoding a novel patatin domain- containing protein, is induced by fasting and glucocorticoids: Ectopic expression of desnutrin increases triglyceride hydrolysis. *The Journal of Biological Chemistry*, *279*, 47066–47075. https://doi.org/10.1074/jbc. M403855200

Wang, L., Schmitz, V., Perez-Mediavilla, A., Izal, I., Prieto, J., & Qian, C. (2003). Suppression of angiogenesis and tumor growth by adenoviral- mediated gene transfer of pigment epithelium-derived factor. *Molecu- lar Therapy*, *8*, 72–79.

Wang, X., Liu, X., Ren, Y., Liu, Y., Han, S., Zhao, J., … He, Y. (2019). PEDF protects human retinal pigment epithelial cells against oxidative stress via upregulation of UCP2 expression. *Molecular Medicine Reports*, *19*, 59–74. https://doi.org/10.3892/mmr.2018.9645